



## Detection of pneumoperitoneum in the abdominal radiograph images using artificial neural networks

Mimi Kim<sup>a,1</sup>, Jong Soo Kim<sup>b,\*</sup>, Changhwan Lee<sup>c</sup>, Bo-Kyeong Kang<sup>a</sup>

<sup>a</sup> Department of Radiology, Hanyang University Seoul Hospital, Seoul, Republic of Korea

<sup>b</sup> Institute for Software Convergence, Hanyang University, Seoul, Republic of Korea

<sup>c</sup> Department of Biomedical Engineering, Hanyang University, Seoul, Republic of Korea

### HIGHLIGHTS

- The purpose of this study was to assess the diagnostic performance of artificial neural networks (ANNs) to detect pneumoperitoneum in abdominal radiographs for the first time.
- This approach applied a novel deep-learning algorithm, a simple ANN training process without employing CNN, and also used ResNet-50, for comparison.
- By applying ResNet-50 to abdominal radiographs, we obtained an area under the ROC curve (AUC) of 0.916 and an accuracy of 85.0 % with a sensitivity of 85.7 % and a predictive value of the negative tests (NPV) of 91.7 %.
- Compared with CNN, our novel approach used extremely small ANN structures and a simple ANN training process. The diagnostic performance of our approach, with a sensitivity of 88.6 % and NPV of 91.3 %, was compared decently with that of ResNet-50.

### ARTICLE INFO

#### Keywords:

Abdominal image  
Artificial neural network  
Deep learning  
Pneumoperitoneum

### ABSTRACT

**Background/purpose:** The purpose of this study was to assess the diagnostic performance of artificial neural networks (ANNs) to detect pneumoperitoneum in abdominal radiographs for the first time.

**Materials and methods:** This approach applied a novel deep-learning algorithm, a simple ANN training process without employing a convolution neural network (CNN), and also used a widely utilized deep-learning method, ResNet-50, for comparison.

**Results:** By applying ResNet-50 to abdominal radiographs, we obtained an area under the ROC curve (AUC) of 0.916 and an accuracy of 85.0 % with a sensitivity of 85.7 % and a predictive value of the negative tests (NPV) of 91.7 %. Compared with the most commonly applied deep-learning methods such as a CNN, our novel approach used extremely small ANN structures and a simple ANN training process. The diagnostic performance of our approach, with a sensitivity of 88.6 % and NPV of 91.3 %, was compared decently with that of ResNet-50.

**Conclusions:** The results of this study showed that ANN-based computer-assisted diagnostics can be used to accurately detect pneumoperitoneum in abdominal radiographs, reduce the time delay in diagnosing urgent diseases such as pneumoperitoneum, and increase the effectiveness of clinical practice and patient care.

### 1. Introduction

Pneumoperitoneum, which means free air inside the peritoneum except pneumoretroperitoneum, is an acute abdominal condition such as a gastrointestinal perforation, frequently requiring rapid medical or surgical intervention [1–3]. Therefore, a quick and accurate diagnosis is essential. Diagnosis of acute abdominal pain usually begins with

abdominal radiography recommended by the American College of Radiology [4,5]. However, the interpretation is often obtained slowly, because of the low sensitivity, limited time and manpower, and lower priority compared to other tests such as ultrasound, computed tomography (CT), and magnetic resonance imaging (MRI) [6]. However, abdominal radiographs still have the advantage of a relatively low radioactivity of 0.7 mSv, compared to an average effective CT dose of 8

\* Corresponding author at: Institute for Software Convergence, Hanyang University, 222 Wangsimni-ro, Seongdong-gu, Seoul, 04763, Republic of Korea.

E-mail addresses: [bluefish010@naver.com](mailto:bluefish010@naver.com) (M. Kim), [jongkim57@hanyang.ac.kr](mailto:jongkim57@hanyang.ac.kr) (J.S. Kim), [lchw711@hanyang.ac.kr](mailto:lchw711@hanyang.ac.kr) (C. Lee), [msbbogri@naver.com](mailto:msbbogri@naver.com) (B.-K. Kang).

<sup>1</sup> These authors contributed equally to this work.

mSv, and a follow-up of abdominal distension, bowel obstruction or non-obstructive ileus [7,8].

Deep-learning technology has emerged as an alternative solution to difficult scientific and technical problems. Promising results have been found in the medical image analysis, including diabetic retinopathy in fundus photographs, the detection of metastases in pathological images, and classification of skin cancer in skin radiographs [9–11]. Therefore, this technology could be an alternative to prioritize abdominal radiographs and screen patients, providing a quick response to patients with poor clinical conditions such as suspected pneumoperitoneum in clinical/surgical wards, while being able to overcome generally poor visual diagnostic performance of humans, especially when image quality is degraded due to technical issues such as large patients, improper patient positioning, abdominal overlap of disturbing structures, etc. Recent studies [12–14] have shown the capabilities of a convolution neural network (CNN) based computer-assisted diagnosis of acute chest and abdominal conditions. However, there have been no previous studies using artificial neural networks (ANNs) to detect pneumoperitoneum in abdominal radiographs. Using a deep-learning method, the automatic detection of pneumoperitoneum can help with a preliminary diagnosis and reduce time delays.

A novel deep-learning algorithm for use with ANNs, namely the Kim-Monte Carlo algorithm [15], has recently been reported to be completely different from the back-propagation method [16–18]. The corresponding author (J.S. Kim) has developed the algorithm, which imitates the biological evolution of animals that adapt to a given environment according to the principle of the survival of the fittest. The purpose of this study was to investigate the diagnostic performances of various small ANN models for detecting pneumoperitoneum in abdominal radiographs using a simple training process, the novel deep-learning algorithm, without using CNN which is the most commonly used deep-learning method for image recognition. The dependence of diagnostic performance in detection of pneumoperitoneum in abdominal radiographs on the resolution of input images to an ANN was also studied. In addition, the widely utilized deep-learning method, ResNet-50 [19], was also applied to the same dataset for comparison with our novel approach.

## 2. Materials and methods

### 2.1. Subjects

The institutional review board (IRB) of Hanyang University Seoul Hospital (Seoul, Republic of Korea) approved this study, and confirmed that all methods in this study were performed in accordance with the Good Clinical Practice guidelines with the need for informed consent waived (IRB No. HYUH 2020-03-004).

A total of 1000 clinical grayscale abdominal radiographs of an upright posture obtained between November 2018 and October 2019 were randomly selected from a picture archiving and communication system. The search terms “pneumoperitoneum” and “free air” were used. Two board-certified radiologists (M. Kim and B.K. Kang), with 9 and 13 years of experience in abdominal imaging, respectively, reviewed abdominal radiographs with a consensus of the presence of pneumoperitoneum in all abdominal images. This was confirmed by the presence of pneumoperitoneum based on simultaneous CT or a history of recent abdominal surgery. Patients who recently had undergone surgery with surgical clips were excluded from the analysis to prevent possible contamination. The review results were used as the training data (80 %) for ANN training, and the test data (20 %) was used as a reference for comparison with the pneumoperitoneum detection results of various ANN models.

The experimental data consisted of 346 cases with pneumoperitoneum and 654 normal cases. One thousand patients were randomly divided into 800 cases for the training set and 200 cases for the test set. The training set of 800 cases consisted of 276 cases with pneumoperitoneum and 524 normal cases. The test set of 200 cases

consisted of 70 cases with pneumoperitoneum and 130 normal cases.

### 2.2. Structures of ANN models

To find an extremely small ANN structure that has a diagnostic performance comparable to that of a state-of-the-art deep-learning technology such as a CNN, input image resolution and number of hidden layers of the ANN model started at  $16 \times 20$  and 1, respectively, and were gradually increased [20] for comparing the performance with other ANN models.

Because the size and aspect ratio of the abdominal images were different, all the images were converted into rectangular images with an aspect ratio of 0.9. Thereafter, their pixel resolutions were reduced to  $18 \times 20$ ,  $27 \times 30$ ,  $36 \times 40$ ,  $72 \times 80$ ,  $108 \times 120$ ,  $144 \times 160$ ,  $216 \times 240$ , and  $288 \times 320$ . The number of input nodes of an ANN should be the total number of pixels in the image at a reduced resolution. Therefore, each pixel was converted into black-and-white, and its color value was divided by the maximum value of 255 to achieve a value between zero and 1.0 for use as the input value of an input node [15].

The number of output nodes of the ANN was set to two, i.e., a positive node and a negative node. The target values of the first output node (the positive node, i.e., pneumoperitoneum) and the second output node (the negative node, i.e., normal) were set to 1 and zero, respectively, for the abdominal image with pneumoperitoneum, and *vice versa*. The output value of an ANN for the given input data was obtained using the following formula [20]:

$$\text{value} = (\text{output}[p] - \text{output}[n] + 1) / 2 \quad (1)$$

where  $\text{output}[p]$  and  $\text{output}[n]$  denote the output values of the positive and negative nodes, respectively.

The number of hidden layers of an ANN was set to 1, 2, or 3. The number of nodes in the first hidden layer was set to 20, 40, or 80. Accordingly, 72 small ANN models (= 8 resolutions  $\times$  3  $\times$  3) were constructed.

ResNet-50 [19] was also applied to the same dataset for an input pixel resolution of  $512 \times 512$ . For medical image diagnosis using a CNN, the most commonly used image resolution has been  $512 \times 512$ . Fig. 1 shows a detailed schematic representation of the ResNet-50 structure, showing the actual architecture of the CNN.

### 2.3. ANN and CNN training processes

The novel deep-learning algorithm, “Kim-Monte Carlo” algorithm [15], without the use of a CNN, was applied to train the various small ANN models with the training set as the learning data. The algorithm applies a random optimization process based on a Monte Carlo simulation during the training session to determine the hundreds of thousands or more unknown weight factors and bias values of an ANN with variables that minimize the average training error for the given training data [15]. The initial weight factors and bias values of the ANN were randomly chosen within the range of  $-0.2$  to  $+0.2$  [15]. The algorithm consisted of (a) randomly selecting the weight factors and bias values based on a given selecting ratio of the variables and adjusting their values by small random amounts within the range of  $-0.1$  to  $+0.1$  [15], (b) accepting or rejecting the adjustments depending on whether or not the new values decrease the average training error of the ANN for all training data, and (c) repeating the above two steps [15]. A training session was terminated after 10 repetitions of the training cycle, during which the randomly selecting ratio of the variables of a training cycle was steadily decreased from 15 % to 1.5 % [15] of the total number of variables in the ANN. During the training cycle, the total sum of the randomly selecting ratio of variables was set to 900 %, and 30 attempts were made to adjust the values of the selected variables in small random amounts [20]. After the training session of the ANN with the training set, the test set was applied to the ANN to obtain the test results, including

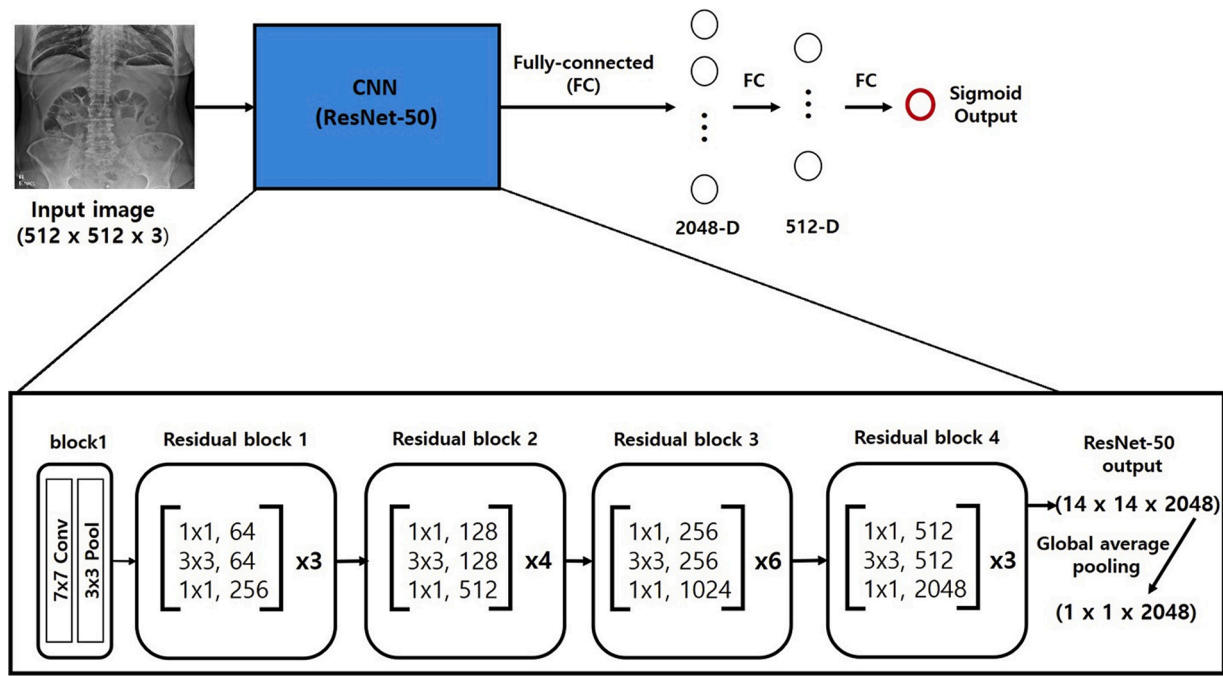


Fig. 1. Schematic representation of ResNet-50 structure.

the output values calculated using Eq. (1), to identify the diagnostic performance of the ANN model. Fig. 2 shows the pipeline for detecting pneumoperitoneum in the abdominal radiograph images using an ANN.

Details about the hardware and software infrastructure to implement the ANNs are described below. The software for ANNs applying the novel deep-learning algorithm was developed and programmed fully in-house by J.S. Kim with Microsoft Visual C++. Regular PCs without graphics processing unit (GPU) computing were used as hardware. The operating system used was Microsoft Windows 10 64-bit professional, and the CPU was Intel i5-7400. The main memory size was 16 GB. The time it took to train an ANN with the training set depended on the size of an ANN structure, and it took 8 h for the ANN structure including 5760

input nodes (i.e.,  $72 \times 80$ ), 40 intermediate nodes in the only hidden layer, and 2 output nodes. It took about a second to predict the entire test set.

ResNet-50 [19] was also applied to the same training set for the input pixel resolution of abdominal images of  $512 \times 512$  (see Fig. 2). Before training, all weight factors were initialized by the Xavier uniform initializer [21]. The CNN was trained using the Adam optimization algorithm [22] with a learning rate of 0.0005. A total of 1000 epochs were executed. Better results were obtained between the lowest training error and all 1000 runs. The hyper-parameters such as the learning rate and the number of epochs applied to ResNet-50 did not change once fixed, and they were determined empirically as optimal values.

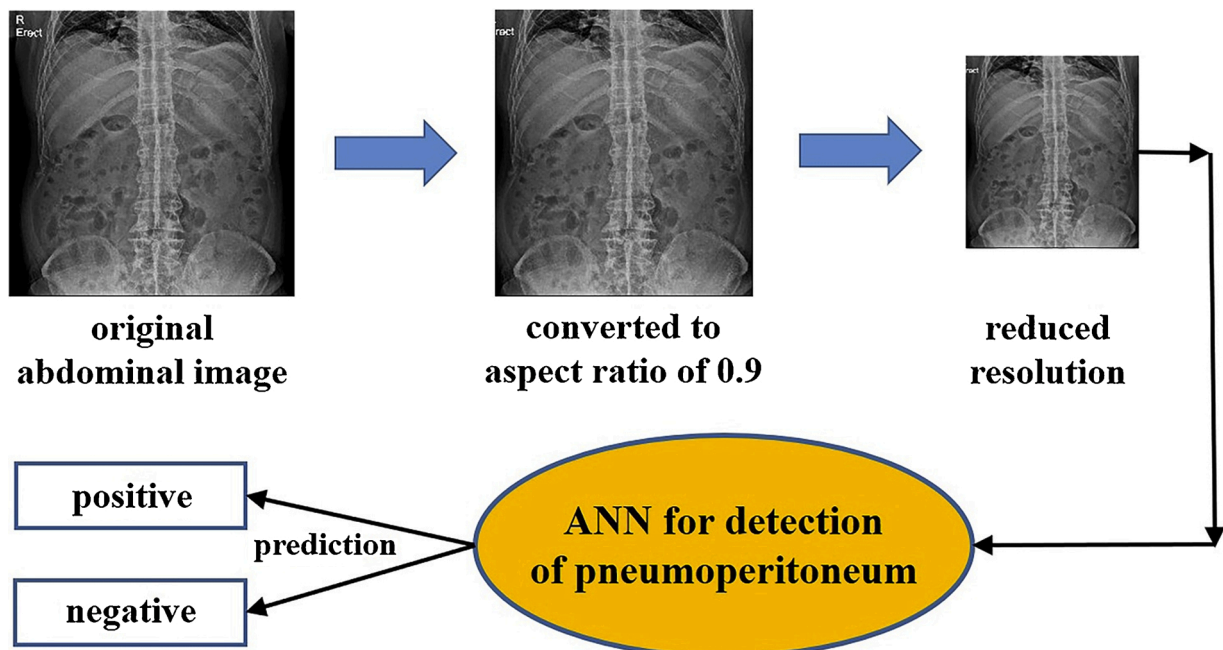


Fig. 2. Pipeline for detecting pneumoperitoneum in the abdominal radiograph images using an ANN.

Class-weighting was added when training ResNet-50. That is, in the training set, there were 524 negative cases and 276 positive cases, and thus, when calculating training error during the training session, class-weights of 1.0 and 1.8985 (= 524/276) were applied for the negative and positive cases, respectively. The results were compared with those trained without class-weighting. However, to compare the performance of the ANNs and ResNet-50 under basic conditions, no additional training techniques, namely, a drop-out or a data augmentation such as image flipping, image zooming in-out, and/or image translation, were applied during the training session.

Details about the hardware and software infrastructure to implement ResNet-50 are described below. The operating system used was Microsoft Windows 10 64-bit professional, and the CPU was Intel i7-4770k. The main memory size was 32 GB, and the GTX 1080 TI graphics accelerator (NVIDIA) with 11 GB RAM (NVIDIA) was used for graphics processing unit (GPU) computing. The deep-learning framework was TensorFlow (version 1.80, Google Brain Team), an end-to-end open source platform for machine learning. Image data was acquired from PACS and the diagnosis system was built externally, i.e., the system was not embedded into PACS. The time it took to train ResNet-50 with the training set was about 17 h. It took a few seconds to predict the entire test set.

### 2.4. ANN training progress

A simple training process was applied to train various small ANN models. Fig. 3 shows a computer screen of the training progress of an ANN. The blue curve denotes the “error rate,” which is the average value of training errors for the entire training set, where the training error is the summation over all the output nodes of the square of the difference between the output value of an output node and the corresponding target value for the given input data [15]. Therefore, the error rate is the absolute criterion of a training in progress. The horizontal value in Fig. 3 indicates the number of successfully changed values of the weight factors and bias values of an ANN during the training session [15].

The red curve in Fig. 3 denotes the “score,” which is the average score for the entire training set, where the score for the given input data is 1.0 if the output node with the maximum output value corresponds to the output node with the maximum target value, and is zero for other cases [15]. The score is equivalent to an accuracy when the cut-off value is arbitrarily set to 0.5 for a receiver operating characteristic (ROC) curve analysis, referring to Eq. (1) [20]. Therefore, the score is a subsidiary reference value of a training in progress.

### 2.5. Statistical analysis

We conducted an ROC analysis to determine and compare the diagnostic performances of various ANN models for detecting pneumoperitoneum. Statistical analyses were applied using commercially available software, SPSS, version 25 for Windows (SPSS, Chicago, IL, USA).

### 3. Results

Table 1 shows the detection results of pneumoperitoneum in abdominal radiographs for the ANN models including 1, 2, or 3 hidden layers with the test set; the results were selected by comparing the test results among the 54 ANN models according to the pixel resolutions of abdominal images, i.e.,  $144 \times 160$ ,  $108 \times 120$ ,  $72 \times 80$ ,  $36 \times 40$ ,  $27 \times 30$ , and  $18 \times 20$  pixels. In Table 1, AUC denotes an area under the ROC curve, PPV indicates a predictive value of the positive tests, and NPV indicates a predictive value of the negative tests. For the ANN structure including 23,040 input nodes (for the input pixel resolution of  $144 \times 160$ ), 20 intermediate nodes in the only hidden layer, and 2 output nodes, we obtained the best diagnostic performance with a sensitivity of 88.6 % and NPV of 91.3 % among the 54 ANN models as presented in Table 1.

Table 1 also lists the detection results of pneumoperitoneum in abdominal radiographs of ResNet-50 trained with and without class-weighting; the test results were compared with those of our novel approach. The diagnostic performance of ResNet-50 trained with class-weighting was not significantly different with that of ResNet-50 trained without class-weighting. As shown at the bottom of Table 1, we obtained an AUC of 0.916 and an accuracy of 85.0 % with a sensitivity of 85.7 % and NPV of 91.7 %.

For the ANN models with the input pixel resolutions higher than  $144 \times 160$ , Table 2 reports the detection results of pneumoperitoneum in abdominal radiographs for the ANN models including 1, 2, or 3 hidden layers with the test set; the results were selected by comparing the test results among the 18 ANN models according to the pixel resolutions of abdominal images of  $216 \times 240$  and  $288 \times 320$ . Comparing Tables 1 and 2, as the pixel resolution increased from  $18 \times 20$ , the diagnostic performance increased and reached the highest value at a pixel resolution of  $144 \times 160$ ; the performance then decreased at higher pixel resolutions of  $216 \times 240$  and  $288 \times 320$ .

### 4. Discussion

Several studies using a CNN-based deep-learning method have been conducted to detect pneumoperitoneum in thoracic X-rays and small

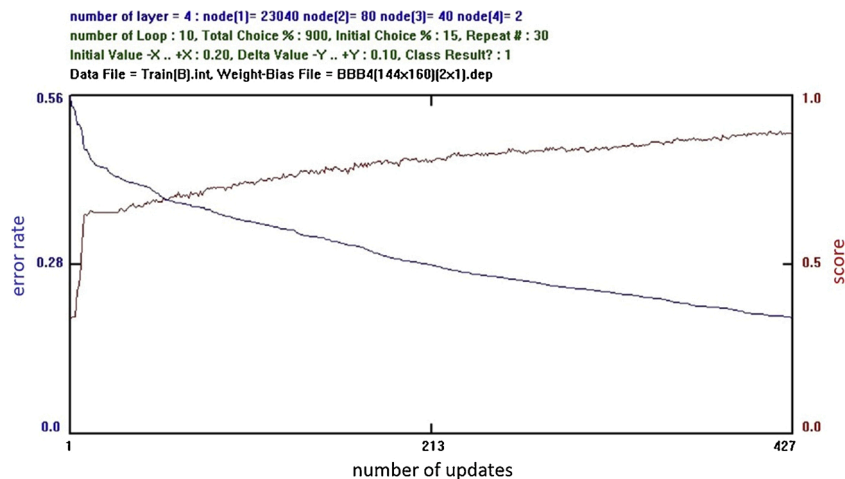


Fig. 3. Computer screen showing the training progress of an ANN.

**Table 1**

Pneumoperitoneum detection results of ANN models including 1, 2, or 3 hidden layers for the input pixel resolutions less than or equal to  $144 \times 160$ , and of ResNet-50 trained with and without class-weighting for the input pixel resolution of  $512 \times 512$ .

Resolution	Hidden nodes	AUC	Cut-off	Sensitivity %	Specificity %	PPV %	NPV %	Accuracy %
$144 \times 160$	20	0.819	0.227	88.6 (62/70)	64.6 (84/130)	57.4 (62/108)	91.3 (84/92)	73.0 (146/200)
$144 \times 160$	20-10-10	0.823	0.199	75.7 (52/70)	75.4 (98/130)	62.4 (53/85)	84.5 (98/116)	75.5 (151/200)
$27 \times 30$	40-20-10	0.779	0.127	68.6 (48/70)	78.5 (102/130)	63.2 (48/76)	82.3(102/124)	75.0 (150/200)
$36 \times 40$	80	0.812	0.497	67.1 (47/70)	83.1 (108/130)	68.1 (47/69)	82.4 (108/131)	77.5 (155/200)
$72 \times 80$	80	0.820	0.405	72.9 (51/70)	81.5 (106/130)	68.0 (51/75)	84.8 (106/125)	78.5 (157/200)
$144 \times 160$	80-40-10	0.790	0.420	61.4 (43/70)	86.9 (113/130)	71.7 (43/60)	80.7 (113/140)	78.0 (156/200)
ResNet-50	with class-weighting	0.870	0.238	84.3 (59/70)	85.4 (111/130)	75.6 (59/78)	91.0 (111/122)	85.0 (170/200)
ResNet-50	without class-weighting	0.916	0.169	85.7 (60/70)	84.6 (110/130)	75.0 (60/80)	91.7 (110/120)	85.0 (170/200)

**Table 2**

Pneumoperitoneum detection results of ANN models including 1, 2, or 3 hidden layers for the input pixel resolutions higher than  $144 \times 160$ .

Resolution	Hidden nodes	AUC	Cut-off	Sensitivity %	Specificity %	PPV %	NPV %	Accuracy %
$216 \times 240$	20	0.774	0.454	68.6 (48/70)	76.2 (99/130)	60.8 (48/79)	81.8 (99/121)	73.5 (147/200)
$216 \times 240$	40	0.794	0.294	77.1 (54/70)	70.0 (90/130)	87.4 (54/94)	84.9 (90/106)	72.5 (144/200)
$216 \times 240$	80-40	0.783	0.544	57.1 (40/70)	87.7 (114/130)	71.4 (40/56)	79.2 (114/144)	77.0 (154/200)
$288 \times 320$	80-40-10	0.753	0.436	60.0 (42/70)	81.5 (105/130)	62.7 (42/67)	78.9 (105/133)	73.5 (147/200)
Average	–	0.776		65.7	78.9	70.6	81.2	74.1

bowel obstructions in abdominal X-rays [12–14], by applying ANNs trained using the back-propagation method [16–18]. Cheng et al. [12] reported that AUCs of high-grade small bowel obstructions were 0.803 based on a set of 2210 abdominal radiographs and 0.971 based on a set of 5558 radiographs. A study was conducted to classify and localize common thorax disease based on chest X-rays [13]. Luo and Chong [14] also applied a CNN-based deep-learning method to detect pneumoperitoneum in thoracic X-rays and small bowel obstructions in abdominal X-rays. However, studies on detection of pneumoperitoneum in abdominal radiographs using ANNs have been scarce.

By applying a novel deep-learning algorithm [15], a simple training process, to various small ANN models for detection of pneumoperitoneum in abdominal radiographs, we obtained a sensitivity of 88.6 % and NPV of 91.3 %. By applying ResNet-50 [19] to the same dataset, the sensitivity was 85.7 % and NPV was 91.7 % as shown in Table 1. Compared to the most commonly used deep-learning methods such as a CNN, our novel approach utilized extremely small ANN structures and a simple training process, and the diagnostic performance was compared decently with that of ResNet-50. The diagnostic performance of an ANN could be significantly improved by applying a larger training dataset and/or applying a data augmentation to the training set such as image flipping, image zooming in-out, and/or image translation.

As the pixel resolution of input images for an ANN increased from  $18 \times 20$ , the diagnostic performance for detecting pneumoperitoneum in abdominal radiographs increased and reached the highest value at  $144 \times 160$ , and the performance then decreased at higher resolutions. Therefore, rather than simply increasing the resolution of input images for an ANN, reducing the input resolution to an appropriate level could yield better results.

Several studies have shown that plain abdominal radiography has a lower diagnostic accuracy of pneumoperitoneum than the other diagnostic modalities. Sensitivity of abdominal radiographs has been reported from 15 % to 78 % [23–25]. This study was the first attempt to detect pneumoperitoneum in abdominal radiographs using ANNs. The diagnostic performance of this study was higher than that reported in previous studies [23–25], particularly in sensitivity and NPV. A screening system of the high sensitivity and NPV can help clinicians to classify patients who need further evaluation and urgent intervention by distinguishing abdominal radiographs with a very low probability of pneumoperitoneum from those may raise suspicion and deserve immediate attention from a radiologist. The entire process of this study can be fully automated and embedded within an abdominal imaging machine; therefore, ANN-based diagnostics can significantly reduce the time

delay of critical diagnosis in real-world situations.

There are several limitations to this study. First, this was a retrospective study with a probable selection bias. Because this study included patients with definitive pneumoperitoneum in abdominal radiographs, a positive bias may occur in the reported statistics. Second, the experimental data included only pneumoperitoneum, and no other abdominal diseases such as small bowel obstructions, renal calculus, and ascites. Finally, there were fewer subjects in a single tertiary hospital. Extensive testing will require further study of large datasets in the future.

In conclusions, a novel deep-learning algorithm, a simple training process, applied to various small ANN models for detection of pneumoperitoneum in abdominal radiographs, showed a fairly good diagnostic performance compared decently with that of ResNet-50. In addition, rather than simply increasing the input image resolution for an ANN, reducing the input resolution to an appropriate value can produce better diagnostic performance for detecting pneumoperitoneum. Finally, this study showed that ANN-based computer-assisted diagnostics can be used to accurately detect pneumoperitoneum in abdominal radiographs with reduced the time delay when diagnosing urgent diseases, such as pneumoperitoneum. It can also increase the efficiency of clinical practice and patient care.

#### Ethical statement

The institutional review board (IRB) of Hanyang University Seoul Hospital (Seoul, Republic of Korea) approved this study, and confirmed that all methods in this study were performed in accordance with the Good Clinical Practice guidelines with the need for informed consent waived (IRB No. HYUH 2020–03-004).

#### CRediT authorship contribution statement

**Mimi Kim:** Conceptualization, Data curation, Formal analysis, Writing - original draft. **Jong Soo Kim:** Conceptualization, Writing - original draft, Writing - review & editing. **Changhwan Lee:** Software, Validation, Visualization. **Bo-Kyeong Kang:** Conceptualization, Data curation, Formal analysis.

#### Declaration of Competing Interest

The authors report no declarations of interest.

## Acknowledgement

This work was supported in part by Hanyang University, Seoul, Republic of Korea (201900000002675).

## References

- [1] C. Chiapponi, U. Stocker, M. Körner, R. Ladurner, Emergency percutaneous needle decompression for tension pneumoperitoneum, *BMC Gastroenterol.* 11 (2011) 48, <https://doi.org/10.1186/1471-230X-11-48>.
- [2] S.C. Fallon, E.S. Kim, B.J. Naik-Mathuria, et al., Needle decompression to avoid tension pneumoperitoneum and hemodynamic compromise after pneumatic reduction of pediatric intussusception, *Pediatr. Radiol.* 43 (2013) 662–667, <https://doi.org/10.1007/s00247-012-2604-y>.
- [3] M. Pitiakoudis, P. Zezos, A. Oikonomou, et al., Spontaneous idiopathic pneumoperitoneum presenting as an acute abdomen: a case report, *J. Med. Case Rep.* 5 (1) (2011) 86, <https://doi.org/10.1186/1752-1947-5-86>.
- [4] M.S. Levine, J.D. Scheiner, S.E. Rubesin, et al., Diagnosis of pneumoperitoneum on supine abdominal radiographs, *Am. J. Roentgenol.* 156 (1991) 731–735, <https://doi.org/10.2214/ajr.156.4.2003436>.
- [5] ACR, Practice Guideline for Digital Radiography, Radiography, AAPM, SIIM, American College of Radiology, Reston, VA, 2007.
- [6] S.H. Ahn, W.W. Mayo-Smith, B.L. Murphy, et al., Acute nontraumatic abdominal pain in adult patients: abdominal radiography compared with CT evaluation, *Radiology* 255 (2002) 159–164, <https://doi.org/10.1148/radiol.2251011282>.
- [7] C.H. Lee, J.H. Kim, M.R. Lee, Postoperative pneumoperitoneum: guilty or not guilty? *J. Korean Surg. Soc.* 82 (4) (2012) 227–231, <https://doi.org/10.4174/jkss.2012.82.4.227>.
- [8] F.A. Mettler, W. Huda, T.T. Yoshizumi, M. Mahesh, Effective doses in radiology and diagnostic nuclear medicine: a catalog, *Radiology* 248 (2008) 254–263, <https://doi.org/10.1148/radiol.2481071451>.
- [9] V. Gulshan, L. Peng, M. Coram, et al., Development and validation of a deep learning algorithm for detection of diabetic retinopathy in retinal fundus photographs, *JAMA - J. Am. Med. Assoc.* 316 (2016) 2402–2410, <https://doi.org/10.1001/jama.2016.17216>.
- [10] A. Esteva, B. Kuprel, R.A. Novoa, et al., Dermatologist-level classification of skin cancer with deep neural networks, *Nature* 542 (2017) 115–118, <https://doi.org/10.1038/nature21056>.
- [11] B.E. Bejnordi, M. Veta, P.J. Van Diest, et al., Diagnostic assessment of deep learning algorithms for detection of lymph node metastases in women with breast cancer, *JAMA - J. Am. Med. Assoc.* 318 (2017) 2199–2210, <https://doi.org/10.1001/jama.2017.14585>.
- [12] P.M. Cheng, K.N. Tran, G. Whang, T.K. Tejura, Refining convolutional neural network detection of small-bowel obstruction in conventional radiography, *Am. J. Roentgenol.* 212 (2019) 342–350, <https://doi.org/10.2214/AJR.18.20362>.
- [13] E.J. Hwang, S. Park, K.N. Jin, et al., Development and validation of a deep learning-based automated detection algorithm for major thoracic diseases on chest radiographs, *JAMA Netw. open* 2 (2019) e191095, <https://doi.org/10.1001/jamanetworkopen.2019.1095>.
- [14] J.W. Luo, J.J.R. Chong, Automated surveillance of chest and abdominal radiographs for acute incidental findings: a deep-learning based approach, *Euro. Soc. Radiol. ECR* 2019 (2019) C-3491, <https://doi.org/10.26044/ecr2019/C-3491>.
- [15] J.S. Kim, Y. Cho, T.H. Lim, Prediction of the location of the glottis in laryngeal images by using a novel deep-learning algorithm, *IEEE Access* 7 (2019) 79545–79554, <https://doi.org/10.1109/ACCESS.2019.2923002>.
- [16] P.J. Werbos, *Beyond Regression: New Tools for Prediction and Analysis in the Behavioral Sciences*, Ph.D. Thesis, Harvard University, Cambridge, MA, 1974.
- [17] D.E. Rumelhart, G.E. Hinton, R.J. Williams, Learning representations by back-propagating errors, *Nature* 323 (1986) 533–536, <https://doi.org/10.1038/323533a0>.
- [18] S. Sathyanarayana, *A gentle introduction to backpropagation*, *Numeric Insight 7* (2014) 1–15.
- [19] K. He, X. Zhang, S. Ren, J. Sun, Deep residual learning for image recognition, *Proceedings of the IEEE Computer Society Conference on Computer Vision and Pattern Recognition* (2016) 770–778, <https://doi.org/10.1109/CVPR.2016.90>.
- [20] J. Lee, J.S. Kim, T.Y. Kim, Y.S. Kim, Detection and classification of intracranial haemorrhage on CT images using a novel deep-learning algorithm, *Sci. Rep.* 10 (2020) 20546, <https://doi.org/10.1038/s41598-020-77441-z>.
- [21] X. Glorot, Y. Bengio, Understanding the difficulty of training deep feedforward neural networks, *J. Mach. Learn. Res.* 9 (2010) 249–256.
- [22] D.P. Kingma, J.L. Ba, Adam: a method for stochastic optimization, *3rd International Conference on Learning Representations, ICLR 2015 - Conference Track Proceedings* (2020) 1–15.
- [23] V. Maniatis, H. Chryssikopoulos, A. Roussakis, et al., Perforation of the alimentary tract: evaluation with computed tomography, *Abdom. Imaging* 29 (2000) 582–589, <https://doi.org/10.1007/s002610000022>.
- [24] A. Van Randen, W. Laméris, J.S.K. Luitse, et al., The role of plain radiographs in patients with acute abdominal pain at the ED, *Am. J. Emerg. Med.* 29 (2011) 582–589, <https://doi.org/10.1016/j.ajem.2009.12.020>.
- [25] S.C. Chen, Z.S. Yen, H.P. Wang, et al., Ultrasonography is superior to plain radiography in the diagnosis of pneumoperitoneum, *Br. J. Surg.* 89 (2002) 351–354, <https://doi.org/10.1046/j.0007-1323.2001.02013.x>.